Journal of Solid State Chemistry 183 (2010) 878–882

Contents lists available at ScienceDirect

Journal of Solid State Chemistry

journal homepage: www.elsevier.com/locate/jssc

Ferromagnetic ordering in $ThSi_2$ type $CeAu_{0.28}Ge_{1.72}$

C. Peter Sebastian, Mercouri G. Kanatzidis *

Department of Chemistry, Northwestern University, 2145 N. Sheridan Road, Evanston, IL 60208-3113, USA

ARTICLE INFO

Article history:
Received 9 December 2009
Accepted 6 February 2010
Available online 15 February 2010

Keywords:
$ThSi_2$ type structure
Kondo behavior
Ferromagnetism

ABSTRACT

The compound $CeAu_{0.28}Ge_{1.72}$ crystallizes in the $ThSi_2$ structure type in the tetragonal space group $I4_1/amd$ with lattice parameters $a=b=4.2415(6)$ Å $c=14.640(3)$ Å. $CeAu_{0.28}Ge_{1.72}$ is a polar intermetallic compound having a three-dimensional Ge/Au polyanion sub-network filled with Ce atoms. The magnetic susceptibility data show Curie–Weiss law behavior above 50 K. The compound orders ferromagnetically at ~8 K with estimated magnetic moment of 2.48 μ_B/Ce. The ferromagnetic ordering is confirmed by the heat capacity data which show a rise at ~8 K. The electronic specific heat coefficient (γ) value obtained from the paramagnetic temperature range 15–25 K is ~124(5) mJ/mol K^2. The entropy change due to the ferromagnetic transition is ~4.2 J/mol K which is appreciably reduced compared to the value of $R\ln(2)$ expected for a crystal-field-split doublet ground state and/or Kondo exchange interactions.

1. Introduction

Intermetallic compounds of Ce exhibit a wide range of physical properties including magnetically ordered Kondo lattice behavior in $CeRhSn_2$ [1,2], heavy fermion behavior in $CeCu_6$ [3], superconductivity in $CeCu_2Si_2$ [4], non-fermi liquid behavior in $CeNi_2Ge_2$ [5], valence fluctuations in $Ce_2Co_3Ge_5$ [6], etc. These unusual properties are associated with the hybridization of the moment carried by the 4*f* electrons with the conduction electrons. Ce can exhibit two electronic configurations: the magnetic Ce^{3+} ($4f^1$) and non-magnetic Ce^{4+} ($4f^0$). In most cases, the magnetic moments derive from Ce^{3+} and order antiferromagnetically at lower temperature. There are several examples, however, that exhibit ferromagnetic order such as CeGaGe [7], CeAgGa [8], CePdSb [9], $CeRu_2Ge_2$ [10], $CeRh_3B_2$ [11].

In the Ce–Au–Ge system [10,12–24], the equiatomic compound CeAuGe crystallizes in the NdPtSb type structure and orders ferromagnetically at 10 K [14,22] while $CeAu_2Ge_2$ [17] adopts the $ThCr_2Si_2$ structure type and orders antiferromagnetically at 16 K [10]. Other notable compounds are Ce_2AuGe_6 (Ce_2CuGe_6 type) [12], $Ce_5Au_xGe_{4-x}$ [x=0.43] [24] which has a Sm_5Ge_4 type structure and $CeAu_{0.75}Ge_{1.25}$ a AlB_2 related compound which orders ferromagnetically at 6 K [19].

During our attempts to synthesize Ce_2AuGe_3, we observed the formation of a mixture of AlB_2-type $CeAu_{0.5+x}Ge_{1.5-x}$ and $ThSi_2$-type $CeAu_{0.5-x}Ge_{1.5+x}$. This was also noticed by Jones et al. [19] but did not report details about the crystal structure and physical properties. A few other ternary systems such as $CeAl_xGe_{2-x}$ [25], $CeCu_xGe_{2-x}$ [26] and $CePd_xGe_{2-x}$ [19] also were reported as mixtures of AlB_2 and $ThSi_2$ type compounds. The wide compositional homogeneity ranges on these systems make it difficult to obtain pure phases for physical property studies. Here we succeeded in obtaining single phase of $ThSi_2$-type $CeAu_{0.28}Ge_{1.72}$ using high frequency induction heating and we report the single crystal structure as well as its magnetic and heat capacity properties.

2. Experimental

2.1. Reagents

The following reagents were used as purchased without further purification. Ce (metal chunk, 99.9%, Chinese Rare Earth Information Center, Inner Mangolia, China), Au (pieces, 99.9% Alfa Aesar, Ward Hill, MA), Ge (ground from 2–5 mm pieces 99.999% Plasmaterials, Livermore, CA).

2.2. Synthesis

$CeAu_{0.28}Ge_{1.72}$ was obtained by combining 0.71 mmol of the cerium metal, 0.2 mmol of gold, 1.25 mmol of germanium. The reactants were sealed in tantalum ampoules under an argon atmosphere in an arc-melting apparatus. A total of 230 mg was used for the synthesis. The tantalum ampoules were subsequently placed in a water-cooled sample chamber of an induction furnace (EasyHeat induction heating system, Model 7590), first rapidly heated to ca. 1250 K and kept at that temperature for 10 min.

* Corresponding author. Fax: +1 847 491 5937.
E-mail addresses: s-peter@northwestern.edu (C.P. Sebastian), m-kanatzidis@northwestern.edu (M.G. Kanatzidis).

0022-4596/$ - see front matter © 2010 Elsevier Inc. All rights reserved.
doi:10.1016/j.jssc.2010.02.003

Finally, the temperature was lowered to 1000 K and the sample was annealed at that temperature for another half an hour, followed by quenching by switching off the power supply. The brittle product could easily be separated from the tantalum tube. No reaction with the container was observed. The polycrystalline sample has a metallic silver color and was used for the elemental analyses, structure characterization, and physical property measurements. More than 95 wt% of the desired compound was obtained.

2.3. Elemental analysis

Quantitative microprobe analyses of $CeAu_{0.28}Ge_{1.72}$ were performed with a Hitachi S-3400 scanning electron microscope (SEM) equipped with a PGT energy dispersive X-ray analyzer. Data were acquired with an accelerating voltage of 25 kV and a 60 s accumulation time. The EDS analysis taken on visibly clean surfaces of the samples gave an atomic composition in good agreement with the results derived from the single crystal X-ray diffraction refinement.

2.4. X-ray crystallography

To determine the phase identity and purity, powder X-ray diffraction patterns of $CeAu_{0.28}Ge_{1.72}$ were collected at RT on a CPS 120 INEL X-ray diffractometer with Cu$K\alpha$ radiation, equipped with a position-sensitive detector and were compared to the pattern calculated from the single crystal structure refinement.

The X-ray single crystal intensity data were collected at 100 K using a STOE IPDS 2T diffractometer with graphite-monochromatized Mo$K\alpha$ (λ=0.71073 Å) radiation. The X-AREA (X-RED and X-SHAPE within) package suite was used for the data extraction and integration and to apply empirical and analytical absorption corrections. The atomic coordinates were taken from the $ThSi_2$ structure and refined with SHELXTL program [27]. A stable refinement for $CeAu_{0.28}Ge_{1.72}$ was accomplished only in the tetragonal space group $I4_1/amd$. Data collection and refinement details are given in Table 1. The final atomic positions and equivalent isotropic displacement parameters are given in Table 2, and selected bond distances are listed in Table 3.

Table 1
Crystal data and structure refinement for $CeAu_{0.28}Ge_{1.72}$.

Empirical formula	$CeAu_{0.28}Ge_{1.72}$
Formula weight	320.13
Temperature	293(2) K
Wavelength	0.71073 Å
Crystal system, space group	Tetragonal, $I4_1/amd$
Unit cell dimensions	a = 4.2415(6) Å
	b = 4.2415(6) Å
	c = 14.640(3) Å
Volume	263.38(7) Å^3
Z, Calculated density	4, 8.073 g/cm^3
Absorption coefficient	51.657 mm^{-1}
F(000)	541
Crystal size	100 × 100 × 50 μm
Theta range for data collection	5.00° – 29.04°
Limiting indices	$-5 \le h \le 5$, $-5 \le k \le 5$, $-20 \le l \le 20$
Reflections collected / unique	1069 / 111 [R(int) = 0.0759]
Completeness to θ = 29.04	97.4%
Refinement method	Full-matrix least-squares on F^2
Data / restraints / parameters	111 / 0 / 9
Goodness-of-fit on F^2	1.242
Final R indices [$I > 2\sigma(I)$]	$R1$ = 0.0532, $wR2$ = 0.1127
R indices (all data)	$R1$ = 0.0541, $wR2$ = 0.1122
Extinction coefficient	0.0000(15)
Largest diff. peak and hole	6.431 and −2.055 e.Å^3

$R = \Sigma||F_o|-|F_c|| / \Sigma|F_o|$, $wR = \{\Sigma[w(|F_o|^2 - |F_c|^2)^2] / \Sigma[w(|F_o|^4)]\}^{1/2}$ and $w = 1/(\sigma^2(I)+0.0016I^2)$.

Table 2
Atomic coordinates ($\times 10^4$), equivalent isotropic displacement parameters (Å$^2 \times 10^3$) and anisotropic displacement parameters (Å$^2 \times 10^3$) for $CeAu_{0.28}Ge_{1.72}$.

	x	y	z	U_{11}	U_{22}	U_{33}	U_{eq}	Occ.
Ce	0	7500	1250	1(1)	1(1)	2(1)	1(1)	1
Au	0	2500	2919(1)	6(1)	13(1)	7(1)	8(1)	0.14
Ge	0	2500	2919(1)	6(1)	13(1)	7(1)	8(1)	0.86

U(eq) is defined as one third of the trace of the orthogonalized U_{ij} tensor. The anisotropic displacement factor exponent takes the form: $-2\pi^2[h^2a^2*U^{11}+\cdots+2hka*b*U^{12}]$. $U_{23}=U_{13}=U_{12}=0$.

Table 3
Interatomic distances (Å) in the structure of $CeAu_{0.28}Ge_{1.72}$, calculated with the powder lattice parameters.

Ce:	7	M	3.2349(15)	M:	1	M	2.435(4)
	4	M			2	M	2.4494(19)
					1	Ce	3.2349(15)
					4	Ce	3.2368(8)

All distances of the first coordination spheres are listed. M denotes $Au_{0.28}Ge_{1.72}$.

2.5. Magnetic measurements

Magnetic susceptibility measurements were carried out with a Quantum Design MPMS SQUID magnetometer. Polycrystalline sample of $CeAu_{0.28}Ge_{1.72}$ was loaded without grinding into gelatin capsules, mounted in a plastic straw and affixed to the end of a carbon fiber rod. Temperature dependence data were collected for both zero field cooled (ZFC) and field cooled mode (FC) between 2 and 300 K, with applied field 1G. Field dependent magnetic measurements were acquired at 2, 5, and 20 K with field sweeping from –50 up to 50 kG for $CeAu_{0.28}Ge_{1.72}$. The raw data were corrected for the diamagnetic contribution.

2.6. Specific heat

Heat capacity (C) measurements were performed on selected polycrystalline sample of $CeAu_{0.28}Ge_{1.72}$, by relaxation method using QD-PPMS. The sample was glued to calibrated HC-puck using Apizeon N grease. C was measured in the 2–50 K range with no applied magnetic fields (H). The electronic and phonon contributions derived by fitting the C vs. T plot using the Debye function [28] within the temperature range 15–25 K, well above the ferromagnetic ordering.

3. Results and discussion

3.1. Reaction chemistry

$CeAu_xGe_{1-x}$ was discovered from efforts to synthesize Ce_2AuGe_3 using the metal flux technique [29]. The main products obtained from the flux reactions were the binary $CeGe_2$ [30] and the equiatomic CeAuGe [15] compound. Reactions using high frequency induction heating gave a mixture of $ThSi_2$- and AlB_2-type $CeAu_xGe_{1-x}$ similar to the Jones report [19]. Both phases could easily be identified in the X-ray powder diffraction patterns. Single crystals were selected from the mixture and their crystal

structure was refined. We observed that elemental compositions of crystals with $x \sim 0.4$ or less crystallize in the $ThSi_2$ type (Table 4) and with x higher than 0.6 crystallize in AlB_2 structure type. We also observed both AlB_2 and $ThSi_2$ phases in the samples with $0.4 < x < 0.6$. It is worth to notice that the lattice constants are increased with Au content. The $ThSi_2$ structure is common in intermetallic compounds and often shows a wide range of stoichiometric phases especially in the ternary systems [19,25,26]. After determining the composition range from the selected three different single crystals we targeted the starting composition of $CeAu_{0.25}Ge_{1.75}$ for direct synthesis using induction heating and obtained the pure compound as only $ThSi_2$ type and without any AlB_2 type at least up to the level of the powder XRD detection limit. One of the single crystals from this system was refined as $CeAu_{0.28}Ge_{1.72}$. The compound is stable in air and no decomposition was observed even after several months. Irregular shaped single crystals of this new compound have metallic luster. The elemental analysis of this compound with SEM/EDS gave the composition 34 ± 3 at% Ce : 9 ± 1 at% Au : 57 ± 3 at% Ge which is in excellent agreement with the results obtained from the single crystal refinement.

Table 4
Compositions and the lattice parameters of $CeAu_xGe_{2-x}$.

Composition	Lattice constants	Method of refinement	Reference
$CeGe_2$	$a=b=4.210(2)$ Å, $c=14.182(5)$ Å	Single crystal	[30]
$CeAu_{0.15}Ge_{1.85}$	$a=b=4.227$ Å, $c=14.387$ Å	Powder	This work
$CeA_{u0.28}Ge_{1.72}$	$a=b=4.2415(6)$ Å $c=14.640(3)$ Å	Single crystal	This work
$CeAu_{0.39}Ge_{1.61}$	$a=b=4.245$ Å, $c=14.712$ Å	Powder	This work

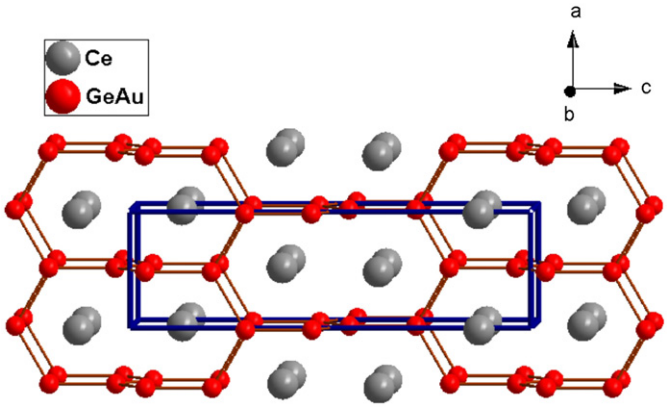

Fig. 1. Crystal structure of $CeAu_{0.28}Ge_{1.72}$ along the b-axis.

3.2. Crystal structure

The crystal structure of $CeAu_{0.28}Ge_{1.72}$ is shown in the Fig. 1 along the b axis. In the $ThSi_2$ structure type [31] the Ce atom occupies Th ($\bar{4}m2$) position while the Si ($2mm$) positions are filled with a mixture of Au and Ge atoms. The compound is isostructural with $CeGe_2$ [30] and is made up of a three-dimensional Ge polyanionic network, with the Ce atoms occupying the voids and channels within it (Fig. 1). The lattice constants are compared with the $CeGe_2$ in Table 4. The Ge–Ge distances are within the range 2.435(4)Å and 2.449(2)Å, are comparable to the Ge–Ge distances in $CeCu_xGe_{1-x}$ (2.396 Å) [26] and $CeAl_xGe_{1-x}$ (2.454 Å) [25] compounds but slightly larger than in $CeGe_2$ (2.355 Å) [30]. The Ge–Ge distances are also comparable to those in elemental Ge indicating the existence of the covalent bonds between the atoms. The shortest distance between the Ce and Ge atoms is 3.235(2)Å which is common in Ce–Ge based intermetallics [25,32–34]. The coordination polyhedra of Ce and M(Au+Ge) are shown in Fig. 2. The M site has 9-fold coordination and is best described as a tri-capped trigonal prism.

3.3. Physical properties

3.3.1. Magnetic susceptibility

Fig. 3(a) shows the temperature dependence of the FC and ZFC molar magnetic susceptibility $\chi_m(T)$ of $CeAu_{0.28}Ge_{1.72}$ sample. The compound shows a long range ferromagnetic ordering below 8 K and no other magnetic transition down to 2 K. The inset displays the inverse molar magnetic susceptibility $1/\chi_m(T)$ data vs. the temperature. Above 50 K, $CeAu_{0.28}Ge_{1.72}$ exhibits paramagnetic behavior and $\chi_m(T)$ nicely follows the Curie–Weiss (CW) law $\chi(T)=C/(T-\theta_p)$ [35], where $C=N_A\mu_{eff}^2/3k_B=\mu_{eff}^2/8$ is the Curie constant and θ_p is the Weiss temperature. Linear least-squares fit to this equation of the data above 100 K resulted in a Weiss temperature of $\theta_p \approx 34$ K suggesting ferromagnetic interactions between the Ce atoms, and an effective moment of 2.48 μ_B/Ce atom. This experimental value is close to that expected for a free Ce^{3+} ion (2.54 μ_B). On the other hand, below 50 K the $\chi_m(T)$ data do not obey the CW law, while below ~8 K there is an sudden

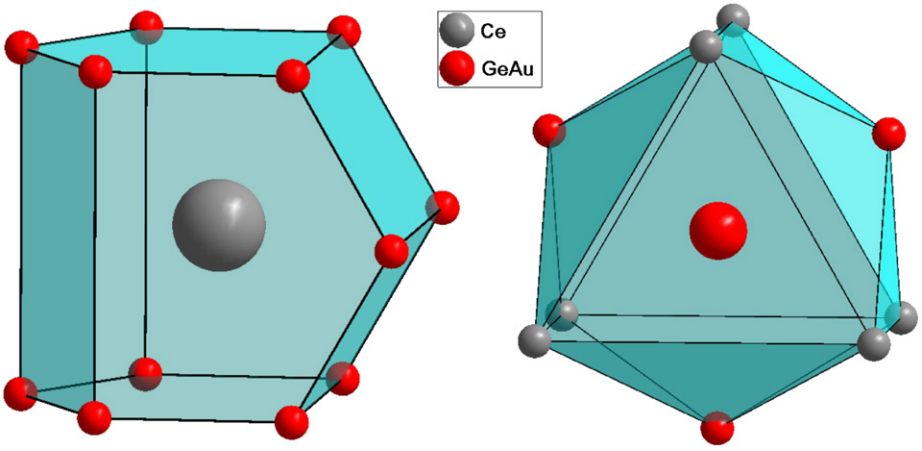

Fig. 2. The coordination polyhedral of Ce and M(Ce+Au) atoms of tetragonal $CeAu_{0.28}Ge_{1.72}$.

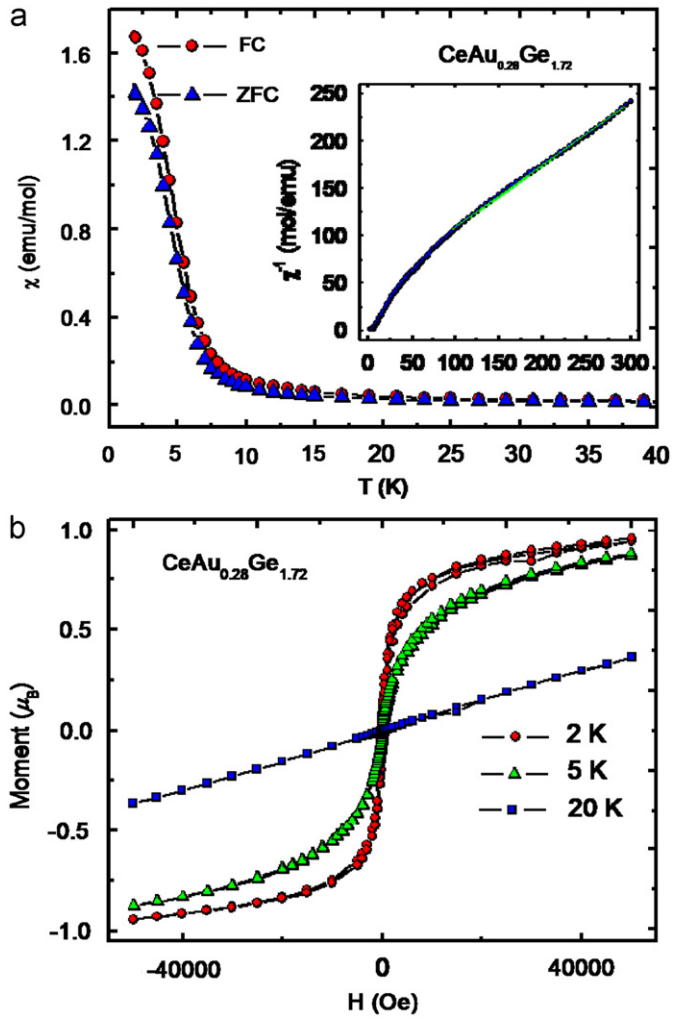

Fig. 3. (a) Field cooled (FC) and zero field cooled (ZFC) magnetic susceptibility (χ=M/H) as a function of temperature for $CeAu_{0.28}Ge_{1.72}$ (polycrystalline) sample measured in a dc field of 1 kOe. Inset shows the temperature dependent inverse susceptibility of $CeAu_{0.28}Ge_{1.72}$. The linear region is marked clearly in the figure. (b) M(H) measured for $CeAu_{0.28}Ge_{1.72}$ polycrystalline sample at various temperatures spanning T_c.

rise in the magnetic moment indicative of ferromagnetic order. The isostructural parent compound $CeGe_2$ shows both antiferromagnetic (T_N=7 K) and ferromagnetic ordering (T_c=4.3 K) at 1000 Oe [36]. The partial substitution of gold in the germanium position suppresses the antiferromagnetic ordering and shifts the ferromagnetic transition to higher temperatures.

Fig. 3(b) illustrates the field dependent magnetization data for $CeAu_{0.28}Ge_{1.72}$ measured at 2, 5 and 20 K. The data measured at 20 K (above the ferromagnetic ordering) exhibit linear behavior and no signs of saturation up to our highest attainable field of 50 kG. The magnetization curve taken at 5 K (within the ferromagnetic ordering) shows a strong field dependent response up to ~5.2 kOe, which almost saturates at ~20 kOe, but continues to rise slowly up to the highest obtainable field (50 kG). At 2 K the strong field dependent on the magnetic moment up to 5 kOe but the system saturates rapidly.

Inside the ordered region (Fig. 3(b)) the magnetization tends to saturate at slightly less than 1 μB/mol Ce at ~25 kG. In spite of the paramagnetic effective moment at higher temperature indicating an unperturbed Ce^{3+} ionic species, the saturation moment is significantly below the theoretical value for Ce (2.54 μB/mol). This may arise from crystal field splitting of the J=5/2 multiplet ground state of the Ce^{3+} ion in this compound as for example in CeAuGe [16] and $CeAgAl_3$ [37], which also show a low saturation moment.

3.3.2. Heat capacity

The temperature dependent specific heat from 1.8 to 50 K for $CeAu_{0.28}Ge_{1.72}$ is shown in Fig. 4(a). There is a rise in C_p at 8 K confirming the magnetic order in this compound. The temperature where the rise in C_p is observed is close to the Curie temperature of 8 K. There is a peak at 4 K, below which the heat capacity drops. The data can be described well by the Debye function [28] in Eq. (1) where the first and second terms correspond to the electronic and the phonon contribution, respectively. N is the number of the atoms in the formula unit and $x=\hbar\omega/k_BT$.

$$C_p(T)=\gamma T+9NR\left(\frac{T}{\Theta_D}\right)^3\int_0^{\Theta_D/T}\frac{x^4dx}{(e^x-1)^2}-KT^3 \quad (1)$$

A fit to the experimental points could only be made within the temperature region 15–25 K, well-above the ferromagnetic ordering and within the paramagnetic state of the material. The fit resulted in a Debye temperature Θ_D of ~184 K and an electronic specific heat coefficient $\gamma \approx 124(5)$ mJ/mol K^2. Because of the inability to include the 2–15 K data in the fit, the estimate γ

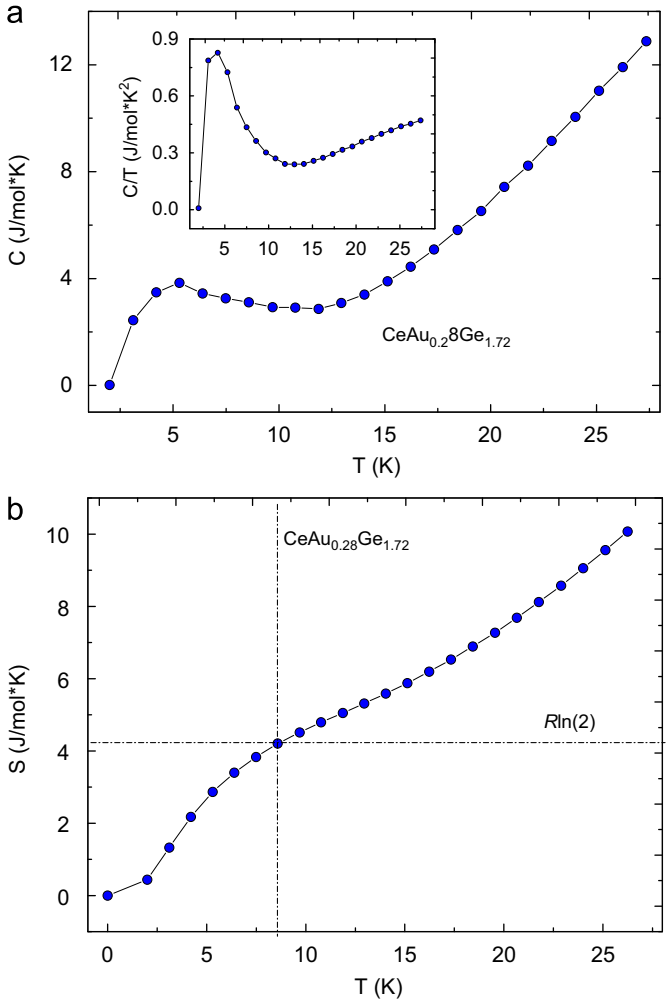

Fig. 4. (a) Heat capacity (C) for $CeAu_{0.28}Ge_{1.72}$ measured as a function of temperature (T) at zero applied fields. The inset figure is C/T vs. T. (b) The total entropy (S) vs. T for $CeAu_{0.28}Ge_{1.72}$ calculated from C measured at zero applied field. The vertical line indicates the ferromagnetic ordering temperature (T_N=8 K) whereas the horizontal line is drawn to show the value of full magnetic entropy for Ce ($R\ln(2J+1)$ for J=1/2).

value may be subject to a large uncertainty. Ferromagnetic correlations are expected to be small in this temperature range since the lower limit of this temperature (15 K) is close to $\sim 2T_c$. The apparently large value of γ could originate from crystal field effects and/or Kondo interactions.

The entropy associated with the magnetic ordering is given by $\Delta S = \int Cp/T\,dT$. In Fig. 4(b), we show the total entropy for $CeAu_{0.28}Ge_{1.72}$, calculated from the C_p/T vs. T plot. It is clear that the total entropy changes at 8 K in accord with the ferromagnetic ordering. For cerium (S-state ion with zero angular momentum and $J=1/2$) the full magnetic entropy ($R\ln 2$) should be recovered just above the ordering temperature. For $CeAu_{0.28}Ge_{1.72}$, the total entropy (S) is not saturated above T_c and increases up to the highest temperature measured, i.e., 50 K without any sign of saturation.

The total entropy gives a value of 4.2 J/mole K over the temperature 7–9 K, where the magnetic ordering occurs. The ΔS obtained is low compared to the value $R\ln(2)=5.75$ J/mol K expected assuming that the Ce ions are in the crystal field split doublet ground state. It is possible that the magnetic entropy is tied up with the magnetic short range order persisting well above the transition temperature in the paramagnetic region. Reduced values of magnetic entropy can also arise from the presence of significant Kondo exchange interactions which may partially quench the local spin [38–40]. Smaller entropy values were also observed for Ce_xAlGe_{2-x} [25].

4. Concluding remarks

Single phase $ThSi_2$-type $CeAu_{0.28}Ge_{1.72}$ was successfully prepared and was found to order ferromagnetically at $\sim$8 K. Above this temperature $CeAu_{0.28}Ge_{1.72}$ obeys Curie Weiss behavior and Ce is in trivalent state. The ferromagnetic interaction between the Ce atoms is also evident in the rise of the heat capacity observed at $\sim$8 K. The estimated enhanced γ ($\sim$124 mJ/mol K^2) value in the paramagnetic range of $CeAu_{0.28}Ge_{1.72}$ could indicate possible heavy fermion behavior or crystal field effect and/or Kondo interaction and needs to be investigated further.

Acknowledgments

Financial support from the Department of Energy (Grant DE-FG02-07ER46356) is gratefully acknowledged. Use was made of facilities operated by the Northwestern Materials Research Center under NSF Grand DMR-0520513. Technical support was provided by Dr. O. Chernyashevskyy.

References

[1] M. Gamza, A. Slebarski, H. Rosner, Journal of Physics: Condensed Matter 20 (2008) 025201–025209.
[2] Z. Hossain, L.C. Gupta, C. Geibel, Journal of Physics: Condensed Matter 14 (2002) 9687–9691.
[3] G.R. Stewart, Z. Fisk, M.S. Wire, Physical Review B 30 (1984) 482–484.
[4] F. Steglich, J. Aarts, C.D. Bredl, W. Lieke, D. Meschede, W. Franz, H. Schafer, Physical Review Letters 43 (1979) 1892–1896.
[5] Y. Aoki, J. Urakawa, H. Sugawara, H. Sato, T. Fukuhara, K. Maezawa, Journal of the Physical Society of Japan 66 (1997) 2993–2996.
[6] S. Layek, V.K. Anand, Z. Hossain, Journal of Magnetism and Magnetic Materials 321 (2009) 3447–3452.
[7] S.K. Dhar, S.M. Pattalwar, R. Vijayaraghavan, Physica B 188 (1993) 491–493.
[8] D.T. Adroja, B.D. Rainford, S.K. Malik, Physica B 188 (1993) 566–568.
[9] S.K. Malik, D.T. Adroja, Physical Review B 43 (1991) 6295–6298.
[10] A. Bohm, R. Caspary, U. Habel, L. Pawlak, A. Zuber, F. Steglich, A. Loidl, Journal of Magnetism and Magnetic Materials 76-7 (1988) 150–152.
[11] S.K. Dhar, S.K. Malik, R. Vijayaraghavan, Journal of Physics C: Solid State Physics 14 (1981) L321–L324.
[12] O. Sologub, K. Hiebl, P. Rogl, O.I. Bodak, Journal of Alloys and Compounds 227 (1995) 37–39.
[13] D. Rossi, R. Marazza, R. Ferro, Journal of Alloys and Compounds 187 (1992) 267–270.
[14] R. Pottgen, H. Borrmann, R.K. Kremer, Journal of Magnetism and Magnetic Materials 152 (1996) 196–200.
[15] R. Pottgen, H. Borrmann, C. Felser, O. Jepsen, R. Henn, R.K. Kremer, A. Simon, Journal of Alloys and Compounds 235 (1996) 170–175.
[16] B.M. Mhlungu, A.M. Strydom, Physica B: Condensed Matter 403 (2008) 862–863.
[17] A. Loidl, K. Knorr, G. Knopp, A. Krimmel, R. Caspary, A. Bohm, G. Sparn, C. Geibel, F. Steglich, A.P. Murani, Physical Review B 46 (1992) 9341–9351.
[18] A. Loidl, G. Knopp, H. Spille, F. Steglich, A.P. Murani, Physica B 156 (1989) 794–797.
[19] C.D.W. Jones, R.A. Gordon, F.J. DiSalvo, R. Pottgen, R.K. Kremer, Journal of Alloys and Compounds 260 (1997) 50–55.
[20] Y. Jeon, B.Y. Qi, F. Lu, M. Croft, Physical Review B 40 (1989) 1538–1545.
[21] B.J. Gibson, W. Schnelle, R. Pottgen, K. Bartkowski, R.K. Kremer, Czechoslovak Journal of Physics 46 (1996) 2573–2574.
[22] B.J. Gibson, R. Pottgen, R.K. Kremer, Physica B 276 (2000) 734–735.
[23] V. Brouskov, M. Hanfland, R. Pottgen, U. Schwarz, Zeitschrift Fur Kristallographie 220 (2005) 122–127.
[24] S. Bobev, E.D. Bauer, Acta Crystallographica Section E: Structure Reports Online 61 (2005) I73–I75.
[25] S.K. Dhar, S.M. Pattalwar, Journal of Magnetism and Magnetic Materials 152 (1996) 22–26.
[26] G. Nakamoto, T. Hagiuda, M. Kurisu, Physica B: Condensed Matter 312 (2002) 277–279.
[27] SHELXTL 5.10; Bruker Analytical X-ray Systems, Inc.: Madison, WI, 1998.
[28] P. Debye, Annalen der Physik 39 (1912) 789.
[29] M.G. Kanatzidis, R. Pottgen, W. Jeitschko, Angewandte Chemie International Edition 44 (2005) 6996–7023.
[30] E.I. Gladyshevskii, Dopovidi Akademii Nauk Ukrainskoi RSR 3 (1959) 294–297.
[31] A. Brown, Acta Crystallographica 14 (1961) 860–865.
[32] U. Rauchschwalbe, U. Gottwick, U. Ahlheim, H.M. Mayer, F. Steglich, Journal of Less-Common Metals 111 (1985) 265–275.
[33] Y.N. Grin, P. Rogl, B. Chevalier, A.A. Fedorchuk, I.A. Gryniv, Journal of Less-Common Metals 167 (1991) 365–371.
[34] A.V. Morozkin, Y.D. Seropegin, A.V. Gribanov, J.M. Barakatova, Journal of Alloys and Compounds 256 (1997) 175–191.
[35] C. Kittel, Introduction to Solid State Physics, seventh ed., Wiley, Hoboken NJ, 1996 p. 426.
[36] C.L. Lin, T. Yuen, P. Riseborough, X.Y. Huang, J. Li, Journal of Applied Physics 91 (2002) 8117–8119.
[37] T. Muranaka, J. Akimitsu, Physica C: Superconductivity and Its Applications 460 (2007) 688–690.
[38] V.H. Tran, Journal of Alloys and Compounds 383 (2004) 281–285.
[39] S.K. Dhar, P. Manfrinetti, A. Palenzona, Y. Kimura, M. Kozaki, Y. Onuki, T. Takeuchi, Physica B 271 (1999) 150–157.
[40] E. Bauer, N. Pillmayr, E. Gratz, G. Hilscher, D. Gignoux, D. Schmitt, Zeitschrift Fur Physik B: Condensed Matter 67 (1987) 205–210.